M. Marjiuan, I. Martinez and F. Garramiola, "A comparison between continuous and hairpin windings for electric traction drives," *2023 13th International Electric Drives Production Conference (EDPC)*, Regensburg, Germany, 2023, pp. 1-8.

DOI: https://doi.org/10.1109/EDPC60603.2023.10372165

A comparison between continuous and hairpin windings for electric traction drives

Marta Marjiuan
eMotor Development
GKN Automotive
20750 Zumaia, Spain
marta.marijuan@gknautomotive.com
ORCID: 0000-0002-0789-3185

Iago Martinez
eMotor Development
GKN Automotive
20750 Zumaia, Spain
iago.martinez@gknautomotive.com
ORCID: 0000-0001-8082-6897

Fernando Garramiola
Electronics and computing Department
Mondragon Unibertsitatea
20500 Arrasate-Mondragón, Spain
fgarramiola@mondragon.edu
ORCID: 0000-0002-2508-3469

***Abstract*— Present change in mobility to vehicle electrification involves highly exigent requirements on product performance and production technologies. In the manufacturing of electric machines, the stator winding is the most challenging and cost demanding process. Within this context, the existing winding technologies need to be optimised to improve their product and process robustness. Axially inserted hairpins are widely used since they present an attractive design for high power and high torque density traction applications. However, the welding of the hairpins is a complex step that leads to high costs of rejects and frequent appearance of faults. Consequently, the radially inserted continuous winding provides a whole new potential for electric powertrains where the manufacturing process can be significantly simplified. This paper introduces a comparison of two flat wire assembly technologies for mass-produced stators: continuous and hairpin windings. Production stages of each winding technology are reviewed. Moreover, main design constraints and challenges of continuous winding motors are exposed. A Finite Element Method (FEM) based performance comparison of two Interior Permanent Magnet Synchronous Machines (IPMSM) with hairpin and continuous winding is presented. The torque, power, torque ripple, losses, Worldwide Harmonised Light Vehicles Test Procedure (WLTP) efficiency and demagnetisation characteristics are analysed. Finally, new design considerations to overcome the limitations and the performance reduction of continuous winding motors are proposed.**

Keywords*— *continuous winding, hairpin winding, electric vehicle, interior permanent magnet synchronous motor, design for manufacturing

I. INTRODUCTION

The ongoing growth on electrification of the worldwide vehicle fleet requires powerful and efficient electric traction drives. In the automotive industry, to enable competitive and cost-effective motors, high productivity and robust manufacturing processes are required. Among all components, the stator is considered the most challenging and expensive manufacturing part, which represents the dominating part of the total electric motor costs [1]. In general, three main steps are required to produce a stator: stator core production, coil winding process and stator impregnation, where the stator winding is the most complex and cost-demanding step. Within this context, the existing winding technologies need to be optimised to improve their product and process robustness [2].

In mass-produced automotive applications, the flat copper wire has almost replaced the round wire winding which is widely used in many industrial applications. Due to its higher thermal conductivity, improved torque density, better insulation capabilities, and more compact size, the flat copper wire winding is an appropriate solution for next generation electric vehicles [3]. Nowadays, the two main flat wire winding variants used in the automotive industry are formed either by hairpin or continuous winding in most novel electrical machine topologies.

Although hairpin winding is an already established technology on the automotive market for traction motors, continuous winding is increasingly gaining popularity [4]. Several companies on the industry have developed their own continuous winding technology motor and it has already been implemented in an E-segment vehicle [5]. A lean manufacturing, and a robust process leads to an interest on investigating the continuous winding as a potential solution. However, some process limitations [6] are also inherent to this technology which need to be tackled through an optimum design for manufacturing approach [7].

This paper presents a comparative study of the implementation of hairpin and continuous windings on an Interior Permanent Magnet Synchronous Machine (IPMSM). Section II describes the manufacturing process characteristics and main complexities of both technologies. In section III, major design constraints of continuous winding are applied and studied with a comprehensive finite element method (FEM) model. Novel design considerations to enhance the continuous winding motor performance are proposed in section IV. Finally, main contributions of this paper are concluded in section V.

II. MANUFACTURING PROCESS

A. Hairpin winding

Hairpin winding technology consists of a series of U-shape coils which are formed and then axially inserted into the stator slots of the motor. It is one of the most popular winding solutions concerning mass production due to its high automation potentials. A step-by-step production process for axially inserted hairpin wires is described in Fig. 1.

First stages in the hairpin winding manufacturing sequence are the straightening of the pins, cutting them to the appropriate length, and stripping the enamel out of the flat wire [8]. Second step involves bending and shaping the conductors into the desired form. According to [9], shaping of hairpins is a complex step due to the rectangular cross section leading to spring-back effect as well as process-related wire insulation damage.

979-8-3503-7049-2/23/$31.00 ©2023 IEEE

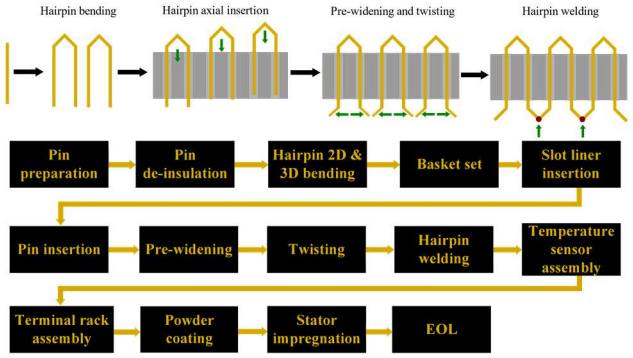

Fig. 1. Axially-insert hairpin winding main production steps

The next steps involve inserting the slot liner in the stator slots and axially inserting the hairpins into the laminated core. Critical damage against slot liner or axial slipping should be avoided during the hairpin insertion. End-winding heads are widened to their final axial and radial position, twisted, and welded according to the specified winding scheme [10]. Then, the welds are protected with an epoxy coating to prevent possible mechanical damage or insulation faults and the stator is impregnated with a varnish. Finally, the end-of-line (EOL) test is performed to verify the overall product functionality.

The most challenging step during hairpin manufacturing sequence is the required welding process [11]. This can result into a very large consuming step, especially with high slot or high conductor-per-slot number. The outcomes of an inappropriate welding process could lead to high costs of rejects, frequent appearance of faults, and heating up the winding due to the increased contact resistance [12].

B. Continuous winding

The continuous winding is a winding design that consists of a series of copper conductors which are shaped and formed into one long mat. This continuous mat is inserted into the stator slots in the radial direction of the electrical machine [13]. Step by step sequence for radial-insert copper conductor assembly is shown in Fig. 2.

First steps involve preparing the copper wire and shaping the mat. Then, the mat is removed from the winding sword and compressed with the aid of two press jaws. Subsequently to forming the continuous winding, the mat is carefully demoulded, wrapped into a carrier tool and compacted.

Preparing the mat and inserting into the lamination stack are the most challenging processes. Once the mat is ready, next step is to insert the winding radially into the stator slots. Special attention should be paid during the mat insertion to avoid damaging the slot liner, scratching the copper insulation, or deforming the conductors leading to higher ohmic resistance [14]

In the radial insertion method, the mat can be inserted by the outer stator diameter or by the inner stator diameter. Depending on the selected winding insertion direction, some design constraints must be considered. For the outer stator diameter insertion, a segmented stator is required (yoke segmentation or yoke-tooth segmentation), whereas, for the inner diameter insertion, an open slot design must be considered.

In the open slot design, a slot wedge is used to close the slot and keep the winding inside in a tight and secure manner. Subsequently, the end windings are welded. This process

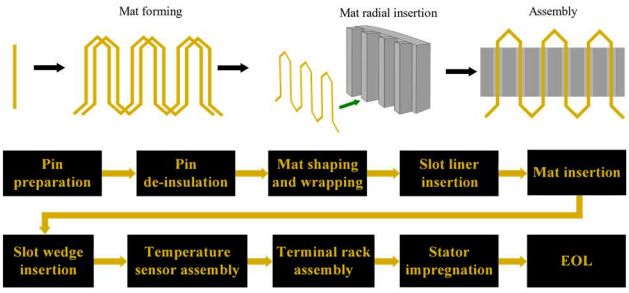

Fig. 2. Radially-insert continuous winding main production steps

requires a lower number of pins to be welded together, given its continuously wound nature. Finally, the stator is impregnated, to improve the heat dissipation, and to mechanically fix the mat and the EOL test is performed.

C. Flat-wire winding technologies comparison

Distributed windings are mainly formed either by hairpin or continuous winding in most automotive electrical machine topologies. Hairpin winding is an attractive design especially for high power and torque density traction applications. As for the continuous winding, it combines the benefits of hairpin technology with round wire, providing a whole new potential for electric powertrains. A comparison between the two rectangular wire assembly methods is described in TABLE I.

Manufacturing complexity is simplified in the continuous design by lowering the number of welding points, avoiding epoxy coating on the coating terminals, and reducing the number of productions stages as well as the number of the pin references to be manufactured. Smaller end-winding heads can also be achieved, leading to an improved compactness and a reduced raw material usage [15]. Additionally, it improves the sustainability due to the easily replaceable winding during electrical machine recycling or repurposing.

The clear advantage of the continuous winding technology relates to high number of slots and high conductors per slot applications. Higher number of turns in series per phase can be achieved compared to hairpin winding, which allows reducing the required inverter currents for high voltage applications. Moreover, it could lead to a higher pole number, decreasing the core back and leading to more power dense designs. Due to the lower current and the lower conductor height, AC copper losses can also be greatly reduced [16]. Nevertheless, a balance between number of conductors per slot and the filling factor reduction should be considered to avoid lowering the machine thermal capacity.

A major shortcoming of the continuous winding is the insertion of the conductors into the stator slots since segmented stator layouts or open slots designs need to be considered. In the stator segmentation, low tolerances are required to avoid degrading the motor performance due to high mechanical stresses and parasitic air gaps between paring components [17]. This involves higher manufacturing costs and higher number of parts to be assembled. In the open slot design, the absence of tooth-tips decreases the motor performance due to lower magnet flux linked through the coils, higher torque ripples and higher acoustic noise. It also leads to higher equivalent air gap lengths, worsening the harmonic content and increasing cogging torque due to the permeability variation of the stator core [18]. Additionally, compared to hairpin windings, the number of parallel branches is limited due to the continuous winding mat nature.

TABLE I. HAIRPIN WINDING AND CONTINUOUS WINDING KEY AREAS COMPARISON

Key area	*Characteristics*	*Hairpin winding*	*Continuous winding*
Stator technology	Nº of slots^{++}	✓	✓✓
	Nº of conductors /slot^{++}	✓	✓✓
	Nº of parallel braches^{++}	✓✓	✗
	Nº of turns $^{++}$	✓	✓✓
	End-winding length^{--}	✓	✓✓
Assembly Process	Number of steps^{--}	✗	✓
	Number of welding points^{--}	✗✗	✓✓
	Process flexibility^{++}	✗	✗
Performance	Peak torque density^{++}	✓✓	✗
	Continuous torque density^{++}	✓✓	✗
	Thermal conductivity^{++}	✓✓	✓✓
	Efficiency at high speed^{++}	✓	✓✓
	NVH, Torque ripple^{--}	✓	✗✗

$^{++}$ Greater is better; $^{--}$ Lower is better.

III. CONTINUOUS AND HAIRPIN WINDING MOTORS PERFORMANCE COMPARISON

A. *Continuous winding design constraints*

Continuous winding presents several process limitations which are inherent to this technology and need to be considered during the design stage. Most of them are related to the mat preparation, shaping, and insertion, which are the most challenging steps.

Following, main design constraints are outlined:

- Open slots or segmented stator designs need to be considered to allow the radial insertion of the mat.
- The flat wire aspect ratio (tangential direction over radial direction) should be below a minimum limit to enable rolling the mat on the inner insertion tool and avoid conductor deformation on the pressing process.
- The flat wire aspect ratio should be above a minimum limit according to the standard IEC 60317-0-2-2013 to ensure the copper wire manufacturability.
- The thinner the flat wires, the better for the mat forming in the sword. However, a minimum manufacturable conductor thickness dimension should be considered according to the standard IEC 60317-0-2-2013.
- The mat insertion tooling dimensions must be considered to size a minimum stator teeth width.
- The stator inner diameter should be above a limit to allow compressing and inserting the mat through the stator open slots while avoiding mechanical interference between adjacent conductors.
- A slot wedge design needs to be considered in open slot stators to mechanically fix the winding in a tight and secure manner inside the slot.
- Appropriate combination of number of slots, poles, and number of turns in series per phase should be designed to produce the mat avoiding complex transpositions and achieve a symmetric winding. Indeed, weak winding symmetries lead to non-desired circulating parasitic currents, especially on highly saturated electric motor [19].

B. *FEM based performance comparative analysis*

A comprehensive performance comparison of two IPMSM with different winding technologies is presented. The base motor is a series production motor for an already industrialised EV application. The aim of this study is to quantify the tooth-tip absence effect on an open slot continuous winding to allow the mat radial insertion on the stator. Based on FEA calculations, torque and power curves, back-EMF, torque ripple, losses, WLTP efficiency and demagnetisation characteristics of both IPMSM are analysed. The hairpin motor's performance is taken as the reference of the normalisation.

1) *Key motor parameters summary*

Key motor parameters are presented in TABLE II. Major difference between the two motor designs is the stator slot shape: the hairpin motor presents semi-closed slots, whereas the continuous winding motor includes open slots.

Both machines have the same rotor design with a single-layer V-shaped magnets concept and the same indirect cooling system has been considered in both cases.

TABLE II. CONTINUOUS AND HAIRPIN WINDING MOTORS KEY PARAMETERS

Motor characteristics	*Hairpin winding motor*	*Continuous winding motor*	*Unit*
Slot design	Semi-closed	Open	
Pole/slot number	8/48		-
Number of conductors per slot	4		
Number of turns in series per phase	16		
Stator outer diameter	210		mm
Stack length	100		mm
Nominal voltage	350		Vdc
Rated current	500		Arms
Rated continuous current	250		Arms

2) *Torque and power performance curves*

In this section, peak and steady-state performance curves are presented (Fig. 3). Same boundary conditions have been defined for both motors: active parts temperature, cooling system conditions and battery voltage level. Maximum speed, output torque and output power results are normalised.

At the MTPA region of the peak performance curve (S2), the continuous winding motor presents a 4% lower torque capacity than the hairpin winding motor. The higher equivalent airgap length and the higher flux leakage on the open slots lead to a lower flux linkage. Considering a motor design optimisation or increasing the phase current could help compensating this lower performance.

On the contrary, in the flux weakening region, the continuous winding motor presents a higher flux weakening ability due to the lower d- and q-axis inductances. At maximum speed, the continuous winding motor shows a 7.9% lower d-axis inductance and a 10.4% lower q-axis inductance

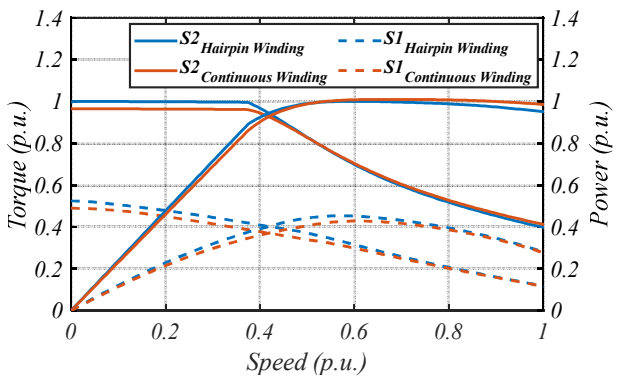

Fig. 3. Peak (S2) and continuous (S1) performance curves comparison at nominal voltage

resulting in to a 3.9% higher output power for the same current and voltage limits.

Similarly, for the steady-state performance (S1), the continuous winding motor shows a 7% lower torque in the low-speed region for the same rated current. However, at high speeds, the same output power is reached due to the required lower d-axis currents in the open slot design to de-flux the motor. Hence, the hairpin winding motor presents an enhanced S2 and S1 performance from 0 to 60% and from 0 to 80% of maximum speed, respectively.

3) Back-EMF

No-load condition has been simulated to evaluate the back-EMF and the cogging torque characteristics. In the continuous winding motor, the presence of slots affects the radial air gap flux density wave form (Fig. 4(a)) and enlarges the Carter's coefficient. This, results in a lower airgap flux density and a lower induced voltage.

The line to line back-EMF waveforms without rotor stacks skew of the two models are shown in Fig. 4(b). Same rotational speed has been considered to enable a reasonable comparison. It is noticeable that in the open slot design, the back-EMF contains a higher harmonic contribution, whilst the semi-closed slot design shows a more sinusoidal waveform. The harmonic spectrum of the back-EMF is shown in Fig. 4(c). The open slot motor presents a 4.9% lower fundamental component of the back-EMF and a 59% higher total harmonic distortion (THD). Indeed, substantial increase can be appreciated in the 5th, 7th, 11th, and 13th harmonics, due to the absence of tooth-tips in the open slot motor.

4) Cogging torque

The cogging torque amplitude in the continuous winding motor is 5 times higher than in the hairpin winding motor. Moreover, the waveform periodicity changes from the closed slot design (7.5º/period, Fig. 5(a)), to the open slot design (45º/period, Fig. 5(b)).

A 6-degree linear skew is applied to the rotor stacks to reduce the motor vibration and noise. In the hairpin motor, the cogging torque improves an 83% from the non-skewed variant. In the continuous winding motor, an 85% torque ripple reduction is achieved which is a 2% higher than hairpin winding motor.

5) Torque ripple

A high harmonic content on the airgap flux distribution, magnetic saturation, and cogging torque are the main causes of torque ripple. To avoid negative impacts on NVH

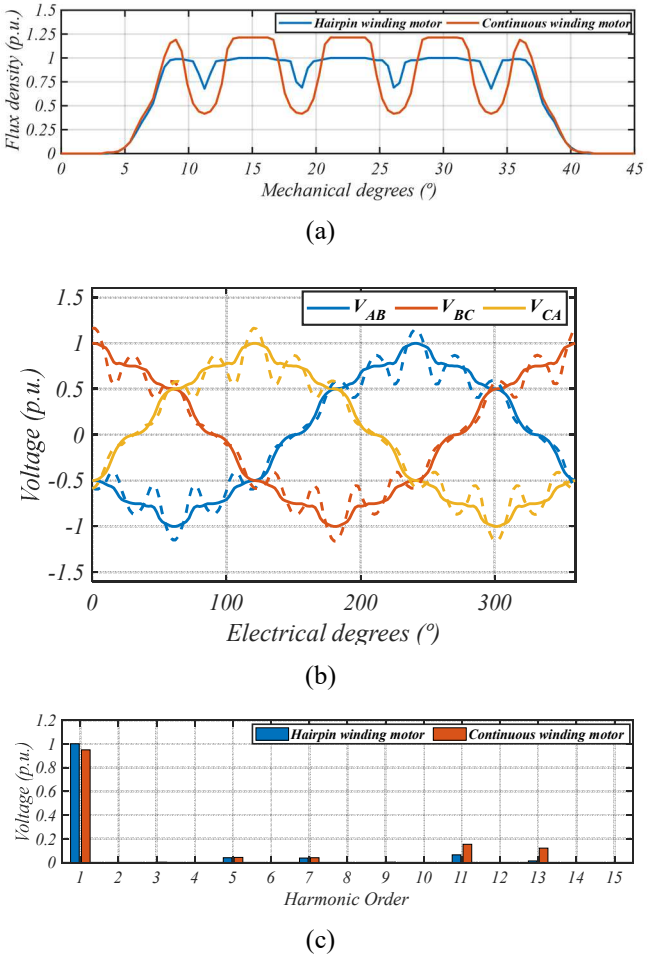

Fig. 4. No-load condition performance comparison. (a) Radial airgap Magnetic Flux; (b) Back-EMF line to line voltage for the hairpin winding motor (solid line) and continuous winding motor (dashed line); (c) Back-EMF harmonic spectrum

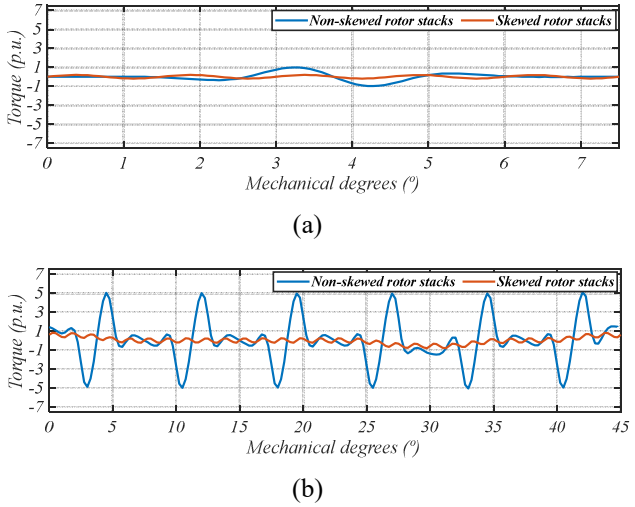

Fig. 5. Skewed and non-skewed rotor stacks cogging torque comparison. (a) Hairpin winding motor; (b) Continuous winding motor

behaviour, torque ripple on all the torque and speed points has been evaluated. The analysis demonstrates that the worst torque ripple condition is located at peak torque and base speed.

The sensitivity analysis in TABLE III. shows that both hairpin and continuous winding motors present unacceptable

TABLE III. TORQUE RIPPLE REDUCTION SENSITIVITY ANALYSIS

Skew Config.	*Skew deg. (º)*	*Number of stacks*	*Hairpin winding motor*		*Continuous winding motor*	
			Torque ripple (%)	*Average torque reduction (%)*	*Torque ripple (%)*	*Average torque reduction (%)*
No Skew	0	1	14.0	0	19.2	-4.0
Linear Skew	4.5	4	8.9	-4.9	8.56	-8.8
	6	5	7.4	-6.2	5.8	-9.7
	7.5	5	5.8	-8.1	4.8	-11.7
V-skew	3	5	12.8	-5.3	10.8	-9.8
	6	5	7.3	-17.3	6.1	-21.4
Zigzag skew	3.75	5	10.5	-5.9	10.1	-8.4

torque ripples values, with maximum torque ripples of 14% and 19%, respectively.

To reduce this torque ripple and improve the motor's high vibration and noise, different skew distributions, skew angles and number of stacks are analysed. In each case, hairpin and continuous winding motor's torque ripple and mean torque reduction are compared.

Linear skew shows the most effective torque ripple reduction with the lowest torque loss. The V-skew presents a lower torque ripple reduction, but it helps reducing the NVH due to lower pulsating axial forces. However, a 3D FEA model should be considered to analyse this effect in detail. In the zigzag skew, the axial flux leakage is too high due to the large skew angles from one stack to the other and the achieved torque ripple reduction is lower than in other arrangements.

In terms of optimum skew angle, a 7.5-degree skew shows the lowest torque ripple. This demonstrates that the highest torque ripple reduction is achieved when the stacks are skewed by a slot pitch angle. In addition, it is evidenced that the rotor skew technique is more effective on the continuous winding motor leading to higher torque ripple reductions in all the analysed cases. For instance, to achieve a 5.8% torque ripple, a 6-degree linear skew is required in the continuous winding motor, whereas a 7.5-degree linear skew in the hairpin design. Hence, despite the open slot motor presents higher initial torque ripples, lower torque fluctuations are achieved by applying the same skew configuration to both motor variants.

6) Losses & efficiency

Copper loss calculation includes proximity and skin effects which are heavily impacted by the motor speed, conductor temperature and the conductor position in the slot. Fig. 6 shows the current density distribution on the flat wires surface. It is evidenced that the current density distribution is less homogenous in the conductors of the continuous winding motor. For instance, at peak torque, maximum speed, and maximum copper temperature (180ºC), the airgap nearest conductor shows 26% higher AC losses in the continuous winding than in the hairpin motor. This leads to 12% higher copper losses in the open slot motor design for this operating point. Besides, as previously described, the required currents are higher in the continuous winding motor leading to higher copper losses in the whole map.

To calculate non-linear iron losses, FEA software is used where Hysteresis, Classical and Excess components are estimated according to Bertotti's loss model. Due to the high local saturations in the closed slot design, the hairpin winding motor presents higher iron losses in the whole torque and speed map. Despite the tooth-tips represent a small area compared to the stator volume, the high harmonics and high saturation of this region lead to large loss concentration in the stator teeth surface (Fig. 7(a)). In the continuous winding case, since tooth-tips are eliminated, local saturations are avoided, and a more balanced magnetic field distribution is achieved (Fig. 7(b)).

A comparison between the difference on the copper losses, iron losses, total losses and efficiency between continuous and hairpin winding motors is represented in Fig. 8. The positive values indicate that the continuous winding motor losses are higher whereas the negative values mean that the hairpin winding motor losses are higher.

The maximum efficiency difference is lower than 1% since copper and iron losses have the opposite effect. In terms of losses, the continuous winding design presents higher losses in almost the whole map, since the copper loss component has a larger influence. However, there is a region at low torque and medium-high speeds, where iron losses have a stronger impact, resulting in higher efficiency values in the continuous winding motor. This is an important outcome, since as explain in the next section, key points of the WLTP cycle are concentrated in this area.

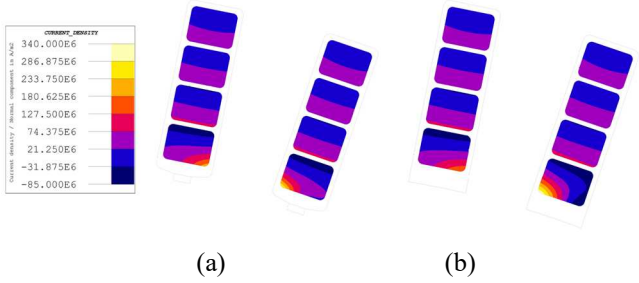

(a) (b)

Fig. 6. Current density distributions at maximum copper temperature, S2-torque and maximum speed point. (a) Hairpin winding motor; (b) Continuous winding motor

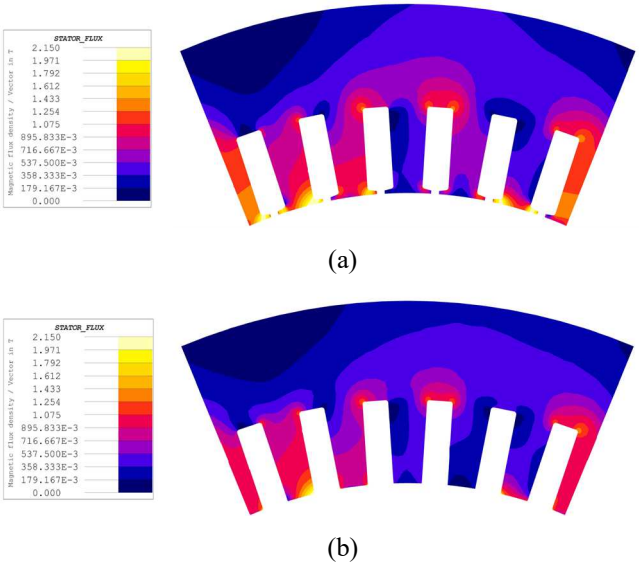

(a)

(b)

Fig. 7. Stator flux density distribution at S2-torque and maximum speed point. (a) Hairpin winding motor; (b) Continuous winding motor

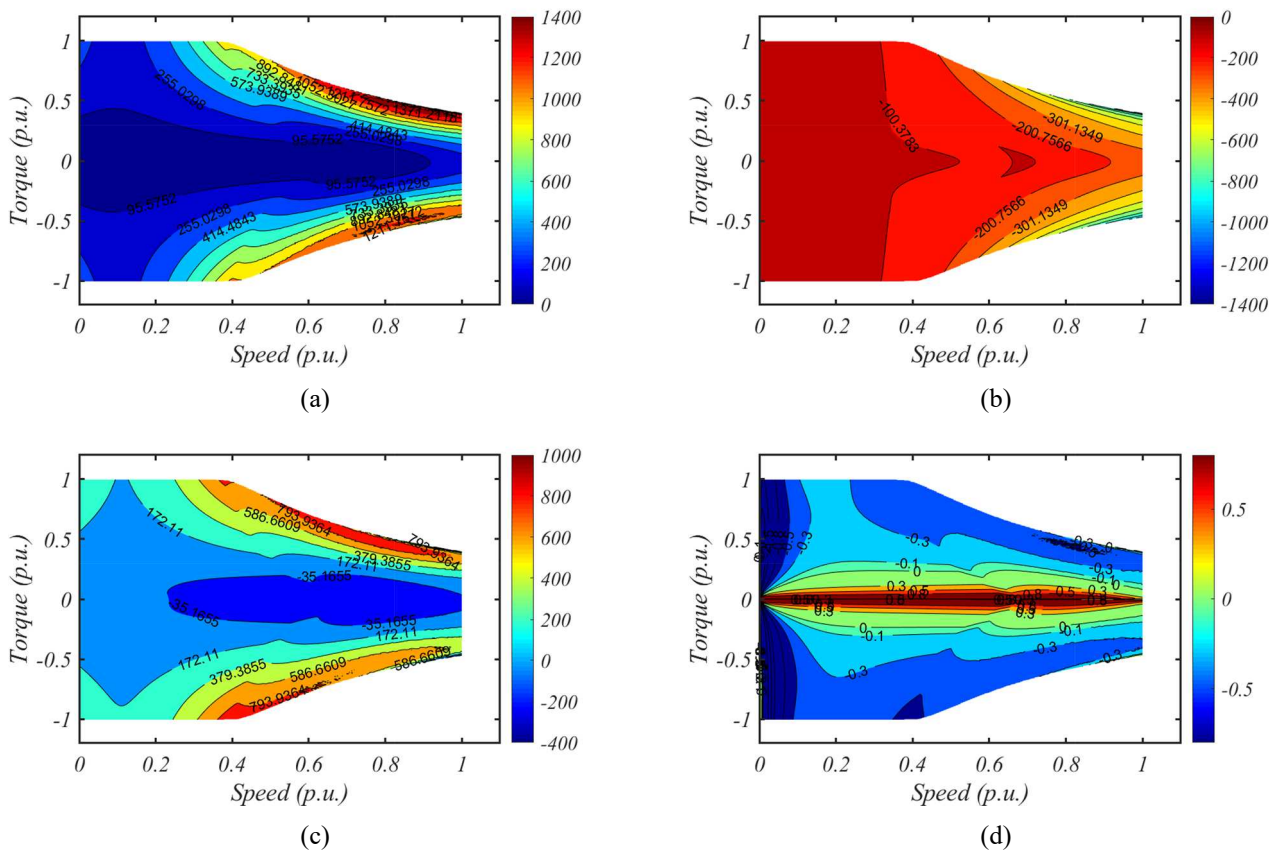

Note: Positive values: Continuous winding motor losses are higher; Negative values: Hairpin winding motor losses are higher

Fig. 8. Continuous and hairpin winding motor losses difference (Continuous- Hairpin). (a) Copper losses; (b) Iron losses; (c) Total losses; (d) Efficiency

7) Efficiency on WLTP cycle

The motor efficiency on the WLTP cycle is a key indicator that needs to be assessed when evaluating an electric vehicle performance. This standard cycle is globally used to determine the electric vehicle range and it is formed by four different sub-parts each one with a different maximum speed. The highest energy consumption on this driving cycle is concentrated at the low torque and high-speed operation region.

The WLTP energy consumption and efficiency of both continuous and hairpin winding IPMSM have been analysed. In both cases, same boundary conditions are considered, for instance, the same B-segment vehicle parameters choice, the gearbox ratio, battery voltage, cooling conditions and active parts temperature.

Since the highest energy loss consumption is concentrated at high-speed area, iron losses have the largest impact on the resulting cycle efficiency. Thus, due to the higher magnetic saturation on the hairpin IPMSM, the continuous winding variant is 0.63% more efficient in the WLTP cycle. As it is shown in TABLE IV., while the copper losses are 10.7% higher in the continuous winding motor, the iron losses are 11.3% lower due to the absence of saturated tooth-tips. Therefore, even if the hairpin winding presents higher maximum efficiency values in almost the whole torque and speed map (Fig. 8(d)), in terms of WLTP efficiency, the continuous winding shows lower consumption rates.

8) Demagnetisation

In this section, the resistance to demagnetisation of continuous and hairpin winding IPMSMs is analysed. To do so, the short-circuit severity is quantified and the performance of the partially demagnetised IPMSM is simulated after a non-desired fault condition.

Firstly, the least favourable condition when a short-circuit could occur is identified and simulated. Among all torque and speed combinations, the worst case is the one with highest generated phase currents, which occurs at the peak torque and base speed point when the maximum steady state magnets temperature is reached.

Next, the generated short-circuit currents are studied. These currents generate a large opposite magnetic field against the magnetizing direction of the magnets, lowering the remanent flux density. The minimum reached flux density value by every magnet finite element is identified and the recoiled new magnetic characteristics are calculated.

As it is shown in TABLE V., for the hairpin motor technology case, focusing on the demagnetised area at 160ºC, it can be noticed that the 7.7% of the magnet volume has crossed the magnetizing knee suffering an irreversible demagnetisation. However, among this 7.7%, only 1.4% of the remaining flux density from the initial magnet remanence has been lost. In other words, as evidenced in Fig. 9, a 7.7% demagnetised magnet surface, results in a 1.4% B_r reduction leading to a 2.9% back-EMF decrease. On the other hand, the

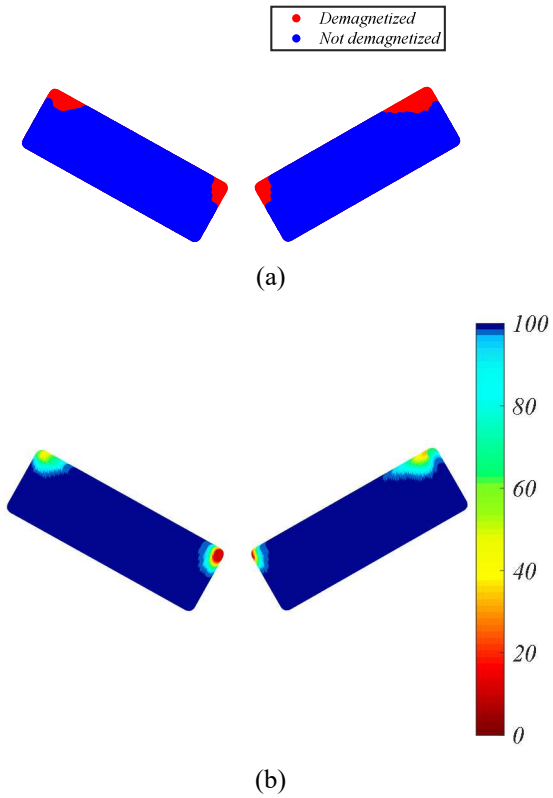

Fig. 9. Partially demagnetised magnets representation. (a) Demagnetisation area; (b) Demagnetised magnet's remaining magnetic flux from the initial Br (%)

same case study for the continuous winding motor presents a 6.4% of demagnetised area, a 1.1% of B_r reduction and a 2.3% of back-EMF decrease. An analogous behaviour is observed at maximum magnets temperature of 180ºC, where the back-EMF reduction of the hairpin is more notorious than the one for continuous winding, reducing a 41.3% and 31.7%, respectively.

It is evidenced that due to the higher magnetic reluctance, the open slot design is more resistant against demagnetisation for the same short-circuit fault condition. Indeed, as demagnetisation severity increases with higher magnet temperatures, the back-EMF reduction difference between both models increases. For instance, the hairpin winding back-EMF reduction is 0.6% higher at 160ºC whereas 9.6% at 180ºC. Hence, a higher Heavy Rare Earth (HRE) reduction could be achieved in a continuous winding motor without lowering its resistance to demagnetisation.

IV. NEW DESIGN CONSIDERATIONS

The improvements on the stator winding manufacturing process should not cause deteriorations on the motor performance. Therefore, to take advantage of the benefits from the continuous winding technology and counter effect its mat insertion related limitations, new design solutions should be investigated. These design solutions do not require advanced manufacturing technologies and can be applicable to mass-produced automotive motors.

A. Magnetic wedges

The open slot associated torque ripple and harmonic content can be effectively reduced with the use of magnetic slot wedges [20]. Indeed, the magnetic slot wedges act as a path for the magnetic field, smoothening the air-gap flux

TABLE IV. WLTP ENERGY CONSUMPTION AND EFFICIENCY RESULTS

WLTP Key Output Data	***Unit***	***Hairpin winding motor***	***Continuous winding motor***
Total energy consumption	kWh/100km	13.25	13.16
Total energy loss	kWh/100km	1.22	1.13
WLTP cycle motor efficiency	%	90.78	91.41 (+0.63%)
Iron losses	Wh	232.18	205.9 (-11.3%)
Copper losses	Wh	47.35	52.42 (+10.7%)

TABLE V. WORST SHORT-CIRCUIT FAULT CONDITION DEMAGNETISATION ANALYSIS

Parameter	***Unit***	***Hairpin winding motor***		***Continuous winding motor***	
Magnet Temperature	ºC	160	180	160	180
B_r reduction	%	1.4	29	1.1	21.7
Demagnetised area	%	7.7	98.4	6.4	97.8
Back-EMF reduction	%	2.9	41.3	2.3	31.7

waveform. An increased relative permeability in the slot section makes the flux more uniformly distributed over the teeth and the wedge surface. However, optimum slot wedge material should be analysed to avoid an increased flux leakage due to high permeability magnetic wedges. Thus, a balance between the optimum magnetic wedge permeability and the torque density should be considered.

B. Increased number of slots

The slot opening width has a large influence in the cogging torque which is mainly generated by the interaction between stator teeth and rotor magnetic field. In addition, the unbalanced air gap flux density produces large slot harmonics and torque ripple, increasing the machine vibration and noise. By increasing the number of slots, the effective slot opening is reduced, the influence of the harmonics is improved, and no advanced manufacturing technologies are required. However, it could cause an efficiency and output torque decrease due to a higher magnetic flux leakage increase though the teeth.

C. Rotor surface optimisation

To shape the rotor polar surface is an effective measure to improve the air gap flux density distribution, and so, to optimise the back-EMF waveform and to reduce the torque fluctuation. Since electrical properties of the machine vary on the path of the magnetic flux produced by the magnets, to apply the flux in the desired direction is a key strategy. One common approach is to include notches in the rotor surface to change the distribution of the gap permeance. Other different method is to use a numerical formula to shape the airgap length such as the inverse cosine function and the advanced inverse cosine function [21]. These equations define the required airgap length to render the airgap flux density sinusoidal. This method would not require additional investment, being suitable for mass-produced electric motors.

D. Rotor stacks skew

One of the most popular techniques to reduce the torque distortion is applying a skew on the rotor stacks. The optimum skewing angle and the minimum number of steps to achieve the best torque ripple reduction should be defined [20]. In this case, no additional geometric complexity is added to the rotor design. On the contrary, higher rotor manufacturing assembly complexity, higher number of references and lower available electromagnetic torque need to be considered.

V. CONCLUSIONS

This paper presents a comparison of two IPMSMs for mass-produced automotive applications with two flat wire assembly technologies: continuous and hairpin windings. Production stages of each technology are described, and continuous winding motors main design constraints and challenges are exposed. In addition, a FEM based comprehensive performance overview of the two motors is provided.

Regarding the manufacturing process, the continuous winding presents a potential solution to replace hairpin stators for mass-produced automotive applications with a lower number of production stages. In terms of performance, the continuous winding motor shows a lower torque capacity due to the tooth-tip absence. Higher torque ripple and worse noise and vibration behaviour are evidenced as well. On the other side, it is found that the tooth-tip absence leads to a better distribution of the flux density in the motor core with lower saturated areas and a more balanced magnetic field distribution. Thereby, lower iron losses and an improved efficiency on the WLTP cycle are evidenced. Moreover, the continuous winding motor presents a higher demagnetisation resistance, and thus, a potential magnets HRE content reduction.

Finally, considering the benefits that the continuous winding technology brings, novel design features to improve the motor performance are proposed. The aim of the selected solutions is to take advantage of the benefits from the continuous winding technology and counter effect its limitations.

REFERENCES

[1] J. Hemsen, N. Nowak, and · Lutz Eckstein, "Production cost modeling for permanent magnet synchronous machines for electric vehicles," *Automotive and Engine Technology 2023 8:2*, vol. 8, no. 2, pp. 109–126, Apr. 2023, doi: 10.1007/S41104-023-00128-W.

[2] I. A. Kampker, B. Dorn, F. Brans, C. Stäck, I. B. Burkhart, and K. Uththama, "Stator design for flexible manufacturing in hairpin technology," *11th International Conference on Power Electronics, Machines and Drives (PEMD 2022)*, pp. 6–11, Aug. 2022, doi: 10.1049/ICP.2022.1002.

[3] S. Xue, M. Michon, M. Popescu, and G. Volpe, "Optimisation of Hairpin Winding in Electric Traction Motor Applications," in *2021 IEEE International Electric Machines and Drives Conference, IEMDC 2021*, Institute of Electrical and Electronics Engineers Inc., May 2021. doi: 10.1109/IEMDC47953.2021.9449605.

[4] A. Kampker, H. H. Heimes, B. Dorn, F. Brans, and C. Stäck, "Challenges of the continuous hairpin technology for production techniques," *Energy Reports*, vol. 9, pp. 107–114, Mar. 2023, doi: 10.1016/J.EGYR.2022.10.370.

[5] "Drive Unit: Motor | Tech Talks | Lucid Motors - YouTube." https://www.youtube.com/watch?v=U7IHZxNC6hc (accessed Apr. 29, 2023).

[6] H. C. Born *et al.*, "Development of a Production Process for Formed Litz Wire Stator Windings," in *2022 12th International Electric Drives Production Conference, EDPC 2022 - Proceedings*, Institute of Electrical and Electronics Engineers Inc., 2022. doi: 10.1109/EDPC56367.2022.10019746.

[7] M. Halwas, L. Hausmann, F. Wirth, J. Fleischer, B. Jux, and M. Doppelbauer, "Influences of design and manufacturing on the performance of electric traction drives," *Proceedings - 2020 International Conference on Electrical Machines, ICEM 2020*, pp. 488–494, Aug. 2020, doi: 10.1109/ICEM49940.2020.9270899.

[8] T. Glaessel, J. Seefried, A. Kuehl, and J. Franke, "Skinning of insulated copper wires within the production chain of hairpin windings for electric traction drives," *International Journal of Mechanical Engineering and Robotics Research*, vol. 9, no. 2, pp. 163–169, Feb. 2020, doi: 10.18178/IJMERR.9.2.163-169.

[9] F. Wirth, T. Kirgor, J. Hofmann, and J. Fleischer, "FE-Based Simulation of Hairpin Shaping Processes for Traction Drives," *2018 8th International Electric Drives Production Conference, EDPC 2018 - Proceedings*, Mar. 2019, doi: 10.1109/EDPC.2018.8658278.

[10] T. Glaessel, J. Seefried, and J. Franke, "Challenges in the manufacturing of hairpin windings and application opportunities of infrared lasers for the contacting process," in *2017 7th International Electric Drives Production Conference (EDPC)*, 2017, pp. 1–7. doi: 10.1109/EDPC.2017.8328150.

[11] A. Riedel *et al.*, "Challenges of the Hairpin Technology for Production Techniques," *ICEMS 2018 - 2018 21st International Conference on Electrical Machines and Systems*, pp. 2471–2476, Nov. 2018, doi: 10.23919/ICEMS.2018.8549105.

[12] J. Vater, M. Pollach, C. Lenz, D. Winkle, and A. Knoll, "Quality control and fault classification of laser welded hairpins in electrical motors," *European Signal Processing Conference*, vol. 2021-January, pp. 1377–1381, Jan. 2021, doi: 10.23919/EUSIPCO47968.2020.9287701.

[13] A. Arzillo *et al.*, "Challenges and Future opportunities of Hairpin Technologies," *IEEE International Symposium on Industrial Electronics*, vol. 2020-June, pp. 277–282, Jun. 2020, doi: 10.1109/ISIE45063.2020.9152417.

[14] T. Glaessel, D. B. Pinhal, M. Masuch, D. Gerling, and J. Franke, "Manufacturing influences on the motor performance of traction drives with hairpin winding," *2019 9th International Electric Drives Production Conference, EDPC 2019 - Proceedings*, Dec. 2019, doi: 10.1109/EDPC48408.2019.9011872.

[15] T. Sayed Hamad, "Quality Assuring of Stator Winding Production," KTH Royal Institute of Technology, Stockholm, Sweden , 2021.

[16] E. Preci *et al.*, "Hairpin Windings: Sensitivity Analysis and Guidelines to Reduce AC Losses."

[17] J. Rens, S. Jacobs, L. Vandenbossche, and E. Attrazic, "Effect of Stator Segmentation and Manufacturing Degradation on the Performance of IPM Machines, Using iCARe® Electrical Steels," *World Electric Vehicle Journal 2016, Vol. 8, Pages 450-460*, vol. 8, no. 2, pp. 450–460, Jun. 2016, doi: 10.3390/WEVJ8020450.

[18] V. Životić-Kukolj and W. L. Soong, "Effect of open stator slots on the performance of an interior permanent magnet automotive alternator," *IET Electr Power Appl*, vol. 7, no. 4, pp. 295–302, 2013, doi: 10.1049/iet-epa.2012.0105.

[19] Christian Du-Bar; Alexander Mann; Oskar Wallmark; Mats Werke, "Comparison of Performance and Manufacturing Aspects of an Insert Winding and a Hairpin Winding for an Automotive Machine Application," *2018 8th International Electric Drives Production Conference, EDPC 2018 - Proceedings*, Mar. 2019, doi: 10.1109/EDPC.2018.8658331.

[20] L. Frosini and M. Pastura, "Analysis and design of innovative magnetic wedges for high efficiency permanent magnet synchronous machines," *Energies (Basel)*, vol. 13, no. 1, Jan. 2020, doi: 10.3390/en13010255.

[21] Y. H. Jung, M. S. Lim, M. H. Yoon, J. S. Jeong, and J. P. Hong, "Torque Ripple Reduction of IPMSM Applying Asymmetric Rotor Shape under Certain Load Condition," *IEEE Transactions on Energy Conversion*, vol. 33, no. 1, pp. 333–340, Mar. 2018, doi: 10.1109/TEC.2017.2752753.